UWB Indoor Path Loss Model for Residential and Commercial Buildings

S.S. Ghassemzadeh[1], L.J. Greenstein[2], A. Kavcic[3], T. Sveinsson[3], V. Tarokh[3]

***Abstract*— We present a statistical model for the path loss of ultra-wideband channels in indoor environments. In contrast to previous measurements, the data reported here are for a bandwidth of 6 GHz rather than 1.25 GHz; they encompass commercial buildings in addition to single-family homes (20 of each); and local spatial averaging is included. As before, the center frequency is 5.0 GHz. Separate models are given for commercial and residential environments and—within each category—for line-of-sight (LOS) and non-line-of-sight (NLS) paths. All four models have the same mathematical structure, differing only in their numerical parameters. The two new models (LOS and NLS) for residences closely match those derived from the previous measurements, thus affirming the stability of our path loss modeling. For greater accuracy, we therefore pool the two data sets in our final models for residences. We find that the path loss statistics for the two categories of buildings are quite similar.**

***Index Terms*—Path Loss, Signal Propagation, UWB.**

I. Introduction

Interest in commercial usage of Ultra-Wideband (UWB) communication systems has increased dramatically since the Federal Communication Commission (FCC) approved UWB transmission from 3.1-10.6GHz [1]. UWB technology is based on transmission of radar like signals with its origin in military applications and short-range radar for tracking and finding. Following the approval of UWB for commercial usage, it is being considered as the physical layer for a new indoor wireless personal area networks (WPAN) standard [2]. The working environment of such networks would be indoor residential and commercial buildings. The propagation channel for UWB signal in such environments is the main focus of this paper.

Indoor signal propagation has been extensively studied over the past two decades, e.g., [3]-[6], although indoor measurements over very wide bandwidths are more recent, e.g., [7]-[12]. Here, we report on the large-scale propagation properties of a UWB channel in both residential and commercial indoor environments. Specifically, we construct a statistical model for the path loss for the environments of interest and conduct simulations confirming its goodness.

The organization of the paper is as follows: Section II covers the implementation of the measurements. Section III gives the basic path loss formula and describes the data reductions. We present the key findings in Section IV. Section V gives the statistical path loss model and the results of our model simulations. Section VI concludes the paper.

II. Measurement Equipment and Database

A. Equipment and Measurement Parameters

We use a network analyzer to transmit 1601 continuous wave tones uniformly distributed from 2-8GHz, with a frequency separation of 3.75MHz. This frequency resolution allows us to capture multipaths with maximum excess delay of 266ns. The 6-GHz wide bandwidth gives a time resolution of 166.7ps.

The hardware setup of the experiment is as follows: The output port of the Power Network Analyzer (PNA) is connected to a 30-dB gain power amplifier (PA). The output power of the PA is returned to the reference port of the PNA to compensate for impedance mismatching between the PNA and PA. The boosted power is also connected to a variable attenuator followed by a conical monopole, 11-GHz wide antenna with linear polarization. We use a conical monopole antenna radiating omni-directionally in the azimuth plane, with 0-dBi gain in the range 1-12GHz. We were able to remove the antenna effects by calibrating the measurement equipment in an anechoic chamber.

A similar antenna receives the signal from the PNA and drives it through a low-noise amplifier (LNA) with a 34dB gain followed by a 45 m long doubly-shielded ultra-low loss coax cable. The output of this cable is then amplified one last time by a 41-dB gain LNA before it is received at input of the same PNA for actual measurement. The measured complex frequency response is stored on a computer hard drive via a GPIB cable controlled by Agilent-VEE programs.

This material is based upon research supported in part by the National Science Foundation under the grant No. CCR-0118701 and Alan T. Waterman award, grant No. CCR-0139398. Any opinions, findings and conclusions or recommendation expressed in this publication are those of the authors and do not necessary reflect the views of the National Science Foundation.

[1] S.S. Ghassemzadeh (saeedg@research.att.com, corresponding author) is with AT&T Labs-Research, Florham Park, NJ, USA.

[2] L.J. Greenstein is with WINLAB-Rutgers University, Piscataway, NJ, USA.

[3] A. Kavcic, T. Sveinsson and V. Tarokh are with Division of Engineering and Applied Sciences, Harvard University, Cambridge MA, USA

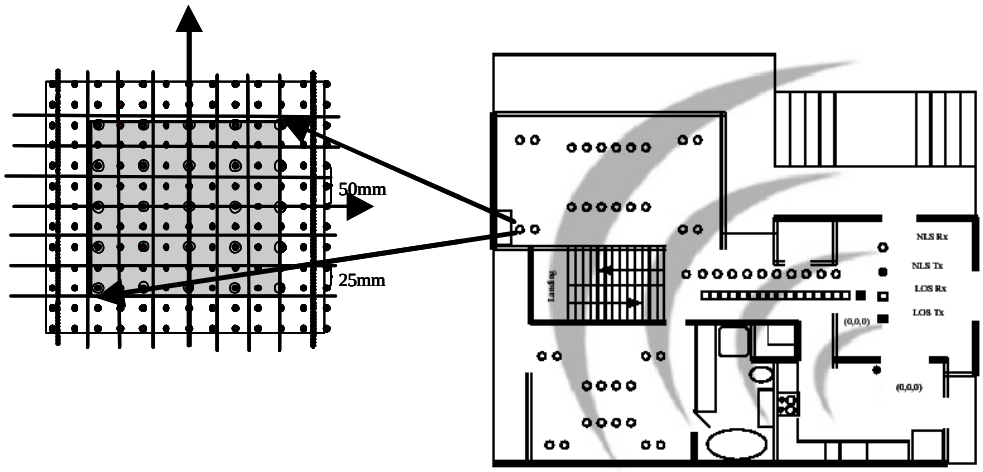

Fig. 1. Illustration of the spatial measurement set-up in a typical building

This set-up was properly calibrated in an anechoic chamber to compensate for the effects of impedance mismatching of the antennas with front-end of the transceiver. The calibration data is also saved for post-processing and reduction of data.

B. Collected Database

The time-invariant nature of the indoor UWB channel has been shown in [10]. Hence, we measured only a single time-snapshot of the channel at each point in space. We captured the small-scale spatial variations by performing spatial measurements around each location, allowing us to construct the local spatial average of channel gain.

We measured 20 commercial buildings and 20 residences in the greater Boston area and in New Jersey. In each building, we selected around 30 locations, with transmitter-receiver (T-R) separation, d, ranging from 0.8 m to 10.5 m for both line-of-sight (LOS) and non-line-of-sight (NLS) paths. We refer to these points as *local points*. Around each local point, we performed 25 spatial measurements on a grid. This is illustrated in Fig.1. We refer to a single point on the grid as a *spatial point*. The distance between spatial points on the grid was 50 mm. Since the highest transmitted frequency has a wavelength of 37.5 mm, the samples are always taken with a separation of at least one wavelength. We performed all the measurements such that the transmitting and receiving antennas are in the same horizontal plane. The height of the antennas was 1.8 m.

III. Path Loss Formula And Data Reductions

A. Path Loss Formula

We define path loss as the dB reduction in power from the transmitter to the receiver location, where the received power is spatially averaged around the location. Specifically it is averaged over an area whose radius is several wavelengths, with the wavelength being that at the center frequency of the transmission. A general path loss formula that incorporates reflection, diffraction and scattering for both LOS and NLS paths can be stated. It has the well-known form

$$PL(d) = PL_0 + 10 \cdot g \cdot \log_{10}(d / d_0) + S \qquad (1)$$

where PL_0 is the point at the reference distance d_0 and g is the slope of the average increase in path loss with dB-distance. The variation S denotes a zero-mean Gaussian random variable with standard deviation s. It can thus be written as

$$S = ys$$

where y is a zero-mean, unit-variance Gaussian random variable. The random variable S is usually referred to as *shadowing*, and it captures the path loss deviation from its median value.

B. Data Reductions

After the removal of stored calibration data, for each local point, the database consists of 25 channel complex frequency responses, $H_k(f_i)$. Here, the index k denotes one of the 25 grid positions and the f_i are 1601 discrete frequencies ranging from 2–8 GHz (i.e., $1 \le k \le 25$ and $0 \le i \le 1600$). We define the spatial *path loss* (in dB) at grid position k and T-R separation d as

$$PL_{sp}^{k}(d) = -10 \cdot \log_{10}\left(\frac{1}{1601} \sum_{i=0}^{1600} \left| H_k(d, f_i) \right|^2 \right) \qquad (2)$$

Note that the spatial path loss is relatively insensitive to frequency and therefore we represent it as an average over all frequencies. Since the database consists of measurements from 25 spatial points around each local point, we compute the local path loss by averaging the corresponding set of spatial path losses. Specifically, we perform the linear average

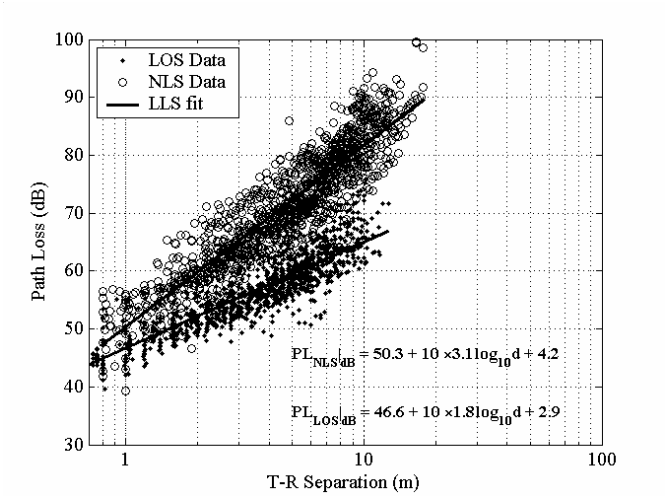

Fig. 2. Path loss vs. T-R separation in residential environments

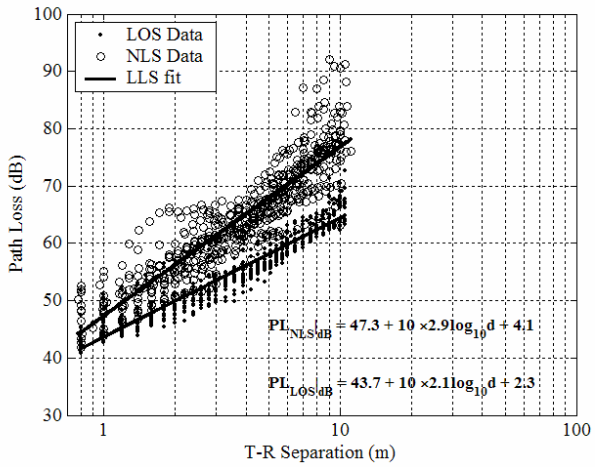

Fig. 3. Path loss vs. T-R separation in commercial environments

$$PL(d) = 10 \cdot \log_{10}\left(\frac{1}{25} \sum_{k=1}^{25} 10^{\frac{PL_{sp}^{k}(d)}{10}} \right) \qquad (3)$$

From each measured frequency response we find the spatial path loss from (2) and the corresponding local path loss from (3). For the remainder of this paper, we work with the latter and refer to it simply as path loss.

IV. Key Findings

We separate our findings into commercial and residential buildings, as well as LOS and NLS paths. For each of the four measured environments, we study the path loss by either pooling data over all buildings or by studying each building separately. Since the center frequency of our measurements is 5 GHz, we expect the path loss values taken from the new homes to be comparable with those of our previous measurements [10]. Recall that the previous measurements were taken in 23 homes over a 1.25-GHz wide frequency band, centered at 5 GHz. The T-R separation of local points ranged from 1 to 15 meters. The path loss values were computed by the same technique as in (2). Later we will increase the statistical fidelity of our database in residential environments by appending the two huge data bases. This will result in a combined database of more than 2000 local path loss points spread uniformly inside 43 homes.

Table I. The path loss parameters over all buildings

Environment	PL_0	g	s
LOS Commercial	43.7	2.07	2.3
NLS Commercial	47.3	2.95	4.1
LOS Residential	45.9	2.01	3.2
NLS Residential	50.3	3.12	3.8

A. Path Loss from All Buildings

Initially, we pool path loss values (computed from the new set of measurements only) from all buildings and study their statistics. Using the linear least squares (LLS) method, we fit (1) to the scatter-plots of path loss $PL(d)$ and T-R separation d (with d_0 = 1 m) and compute PL_0, g and s. Table I summarizes the parameter values for all new measurements. In comparison with results reported in [10] and [11], we noted that the path loss parameters are very similar. Consequently, in our modeling of residential path loss, we will pool the two data bases.

Figure 2 shows scatter plots for LOS and NLS paths in homes (new and previous data pooled), while Fig. 3 shows corresponding scatter plots for commercial buildings (new data only). We see that the main difference between building types is a somewhat higher NLS path loss, on average, in homes. Further measurements in commercial buildings would help test the stability of these results.

Table II. Parameter values in path loss model

Environment	PL_0	m_g	s_g	m_s	s_s
LOS Commercial	43.7	2.04	0.30	1.2	0.6
NLS Commercial	47.3	2.94	0.61	2.4	1.3
LOS Residential	47.2	1.82	0.39	1.5	0.6
NLS Residential	50.4	3.34	0.73	2.6	0.9

B. Path Loss Variation Over Buildings

Differences in building materials, structures and age of buildings cause buildings to exhibit different propagation behaviors. As a result, we expect the slope g and the standard deviation of shadowing, s, to vary among buildings. In fact, in [10], we showed how a statistical path loss model can be created by taking g and s as random variables over buildings while keeping PL_0 fixed. This motivates us to do the same within this work, namely, we fix PL_0 at the mean taken over all buildings, and study the statistics over the pool of extracted g and s.

Table II summarizes the mean and standard deviation of g and s for all environments, along with their corresponding

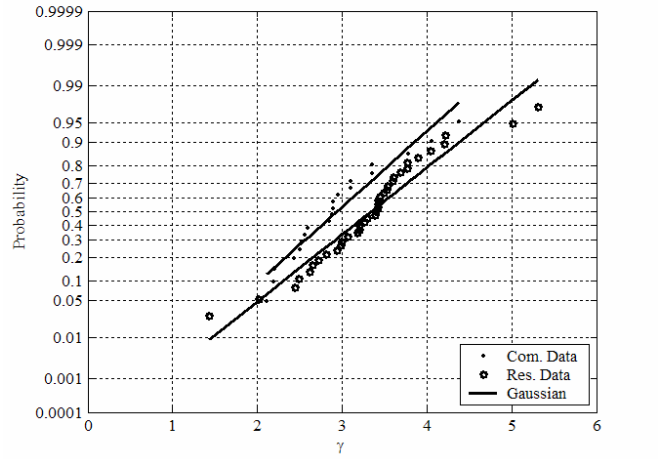

Fig. 4. The distributions of path loss exponent for commercial and residential buildings on NLS paths

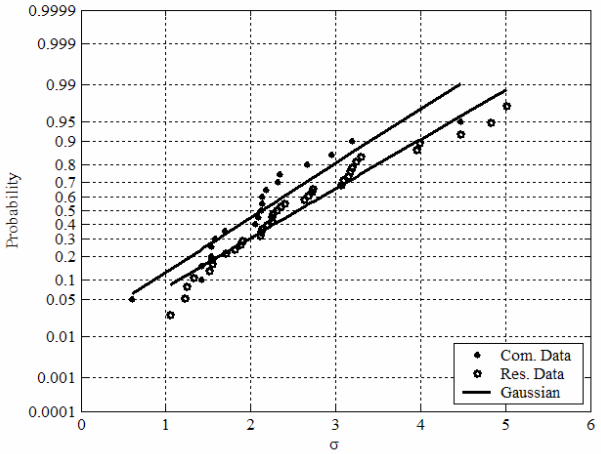

Fig. 5. The distributions of standard deviation of shadowing for commercial and residential buildings on NLS paths

values for PL_0[4]. Figures 4 and 5 show cumulative distribution functions of g and σ, respectively, in commercial and residential buildings on NLS paths. We observe the same behavior on LOS paths. We find the correlation coefficient between g and s in homes to be fairly low (–0.08 and –0.19 for LOS and NLS paths, respectively). Corresponding correlation coefficients for commercial buildings are 0.19 and 0.41 on LOS and NLS paths, respectively.

Finally, we examine the statistics of S, the dB deviation from the median path loss. Figure 6 shows two CDFs for NLS paths, one for all residences and one for all commercial buildings. Similar results are obtained for LOS paths. For residences in particular, we see excellent agreement with the log-normal assumption for shadow fading.

V. The Path Loss Model And Simulations

A. The Path Loss Model

We define a statistical path loss model based on (1), with a fixed intercept point PL_0, but treating g and s as random variables over buildings. Following our key findings, we model all the parameters as independent Gaussian distributions. Note that we could have introduced a new parameter to incorporate the correlation coefficients between g and s into the model (i.e., using Cholesky factorization [13]). However, our earlier simulation results showed little-to-no difference and thus, little justification for adapting a new parameter. Therefore, for simplicity of the model we assume, independence between the parameters g and s.

The Gaussian distribution is completely defined by its first and second moments, allowing us to write

$$\begin{aligned} g &= m_g + s_g \cdot x_1 \\ s &= m_s + s_s \cdot x_2 \end{aligned} \tag{4}$$

where x_1 and x_2 are iid zero-mean, unit-variance Gaussian random variables which vary from building to building. Then we define the complete statistical path loss model as

$$\begin{aligned} PL(d) = & \underbrace{PL_0 + 10 \cdot m_g \cdot \log_{10}(d)}_{\text{Median path loss}} \\ & + \underbrace{10 \cdot s_g \cdot x_1 \cdot \log_{10}(d) + y \cdot m_s + y \cdot x_2 \cdot s_s}_{\text{Deviation from median path loss}} \end{aligned} \tag{5}$$

The deviation from the average path loss is a combination of effects from the two zero-mean, unit-variance Gaussian random variables x_1 and x_2 and the zero-mean, unit-variance Gaussian random variable y. We should emphasize that the random variables x_1, x_2 and y should be selected such that $PL(d)$ does not take unrealistic values. One such way is to use truncated Gaussian distributions (see also [10] and [11]).

B. Simulations

We simulated the path loss model (5) and compared it to that obtained from measurements. For each environment, we

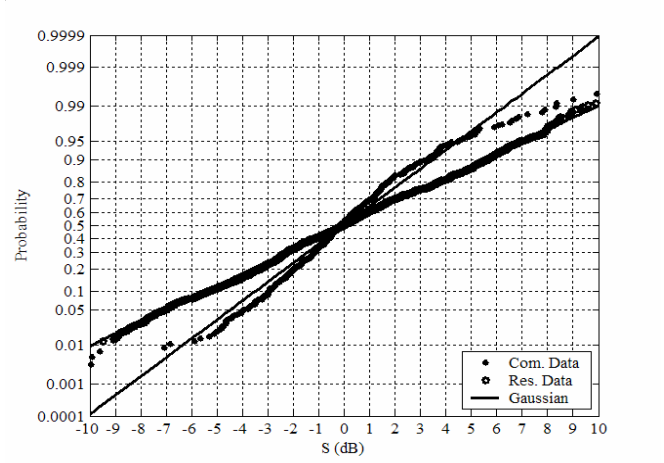

Fig. 6. The shadowing distributions for residential and commercial buildings on NLS paths

[4] Here, we denote the mean and standard deviation of g as m_g and s_g, respectively, and the mean and standard deviation of s as m_s and s_s.

generated 20 realizations of x_1 and x_2, representing the number of measured buildings. We also generated 30 pairs of d and y for each pair of x_1 and x_2, representing the distance and shadowing at each location per building.

Figures 7 and 8 compare simulated and measured scatter plots of NLS path loss in residential and commercial buildings, respectively. We observed similar results for LOS paths. Parameters from the simulations are summarized in Table III and can be compared with those in Table I. The discrepancies are minor. Moreover, recall that the residential data used to obtain Table I were from new measurements only, while the data used to obtain Table III included this database together with the one reported in [10]. This is the cause of most of the differences between these tables. We conclude that our model succeeds in generating path loss statistics very close to those of the database.

Table III. Path loss parameters from simulation

Environment	PL_0	γ	s
LOS Commercial	43.7	2.06	2.6
NLS Commercial	46.8	3.03	3.9
LOS Residential	47.2	1.84	3.0
NLS Residential	50.3	3.29	4.4

VI. Conclusions

We have reported path loss findings from extensive measurements of a wireless UWB channel in 20 commercial buildings and 43 homes. We used a previously proposed statistical path loss model as a basis for modeling the path loss of the channel and confirmed its goodness.

Moreover, the agreement of the current model for residences with those reported in [10] and [11] is excellent. The earlier model was based on measurements over 1.25 GHz, without spatial averaging, and for a different population of homes (or some of the same homes but different paths). The repeatability of the model, combined with its relative simplicity, makes it very useful and reliable for characterizing indoor path loss.

Acknowledgement

The authors thank Dr. Alexander Hiamovich and Dr. Haim Grebel for use of their anechoic chamber at the New Jersey Institute of Technology; Mr. Chris Rice of AT&T Labs-Research, for valuable comments and suggestions on the hardware set-up; and lastly but not least, all the homeowners from AT&T Labs and Harvard University who graciously allowed us to invade their premises with our measurements.

References

[1] FCC Document 00-163: Revision of Part 15 of the Commission's Rules Regarding Ultra-Wideband Transmission Systems, April 22, 2002, ET Docket No. 98-153.

[2] IEEE 802.15.3, IEEE standard for *wireless personal networks* (WPAN), URL: http://www.ieee802.org/15/pub/TG3a.html.

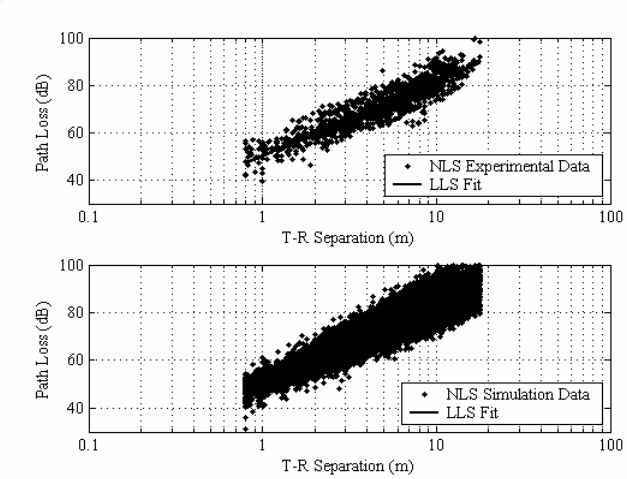

Fig. 7. Path loss: Simulated vs. measured in residential buildings.

[3] A.A. Saleh, R.A. Valenzuela, "A statistical model for indoor multipath propagation", *IEEE J. Sel.. Areas Commun*. 5:128-137, Feb. 1987.

[4] S.J. Howard, K. Pahlavan, "Measurement and analysis of the indoor radio channel in the frequency domain", *IEEE Trans. Instrum. Measure.*, 39:751-755, Oct. 1990.

[5] T.S. Rappaport, S.Y. Seidel, K. Takamizawa, "Statistical channel impulse response models for factory and open plan building radio communication system design", *IEEE Trans. on Commun*., 39:794-806, May 1991.

[6] H. Hashemi, "The indoor propagation channel", *Proc. of the IEEE*, 81:943-968, July, 1993

[7] D. Cassioli, M.Z. Win and A. Molisch, "The ultra-wide bandwith indoor channel: from statistical model to simulations", *IEEE J. Sel. Areas Commun*., 20: pp 1247-1257, Aug. 2002.

[8] J. Foerster, "Channel Modeling Sub-committee Report Final", IEEE P802.15-02/368r5-SG3a.

[9] R. Addler, D. Cheung, E. Green, M. Ho, Q. Li. C. Prettie, L. Rusch, K. Tinsley, "UWB channel measurements for the home environment", *UWB Intel Forum*, 2001 Oregon.

[10] S.S. Ghassemzadeh, et.al. "A statistical path loss model for in-home UWB channels", Proc. *IEEE conf. on Ultra Wideband Systems and Technologies*, pp: 59–64, May 2002.

[11] ————, "Measurement and modeling of an ultra-wideband indoor channel", *IEEE Trans. on Commun*., To appear.

[12] S.S. Ghassemzadeh, L.J. Greenstein , A. Kavcic , T. Sveinsson, V. Tarokh, "UWB indoor delay profile model for residential and commercial buildings", *in Proc. IEEE VTC-Fall 2003*.

[13] C.D. Meyer. "Matrix analysis and applied linear algebra". 2000 SIAM.

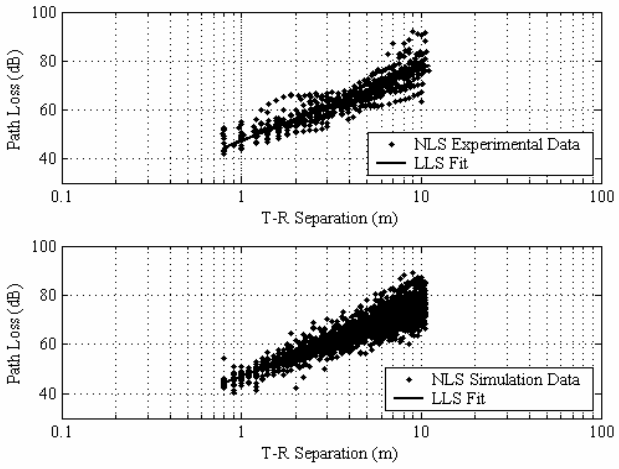

Fig. 8. Path Loss: Simulated vs. measured in commercial buildings.